BIOCHEMISTRY
including biophysical chemistry & molecular biology

Article

pubs.acs.org/biochemistry

Molecular Interactions between Mecamylamine Enantiomers and the Transmembrane Domain of the Human α4β2 Nicotinic Receptor

Vasyl Bondarenko,[†] Katarzyna M. Targowska-Duda,[‡] Krzysztof Jozwiak,[‡] Pei Tang,*[,†,§] and Hugo R. Arias*[,∥]

[†]Department of Anesthesiology, University of Pittsburgh School of Medicine, Pittsburgh, Pennsylvania 15213, United States

[‡]Department of Chemistry, Medical University of Lublin, Lublin, Poland

[§]Department of Computational and Systems Biology and Department of Pharmacology and Chemical Biology, University of Pittsburgh School of Medicine, Pittsburgh, Pennsylvania 15213, United States

[∥]Department of Medical Education, California Northstate University College of Medicine, Elk Grove, California 95757, United States

Supporting Information

ABSTRACT: To characterize the binding sites of mecamylamine enantiomers on the transmembrane domain (TMD) of human (h) $(\alpha4)_3(\beta2)_2$ and $(\alpha4)_2(\beta2)_3$ nicotinic acetylcholine receptors (AChRs), we used nuclear magnetic resonance (NMR), molecular docking, and radioligand binding approaches. The interactions of (*S*)-(+)- and (*R*)-(−)-mecamylamine with several residues, determined by high-resolution NMR, within the hα4β2-TMD indicate different modes of binding at several luminal (L) and nonluminal (NL) sites. In general, the residues sensitive to each mecamylamine enantiomer are similar at both receptor stoichiometries. However, some differences were observed. The molecular docking experiments were crucial for delineating the location and orientation of each enantiomer in its binding site. In the $(\alpha4)_2(\beta2)_3$-TMD, (*S*)-(+)-mecamylamine interacts with the L1 (i.e., between positions −3′ and −5′) and L2 (i.e., between positions 16′ and 20′) sites, whereas the β2-intersubunit (i.e., cytoplasmic end of two β2-TMDs) and α4/β2-intersubunit (i.e., cytoplasmic end of α4-TM1 and β2-TM3) sites are shared by both enantiomers. In the $(\alpha4)_3(\beta2)_2$-TMD, both enantiomers bind with different orientations to the L1′ (closer to ring 2′) and α4-intrasubunit (i.e., at the cytoplasmic ends of α4-TM1 and α4-TM2) sites, but only (*R*)-(−)-mecamylamine interacts with the L2′ (i.e., closer to ring 20′) and α4-TM3-intrasubunit sites. Our findings are important because they provide, for the first time, a structural understanding of the allosteric modulation elicited by mecamylamine enantiomers at each hα4β2 stoichiometry. This advancement could be beneficial for the development of novel therapies for the treatment of several neurological disorders.

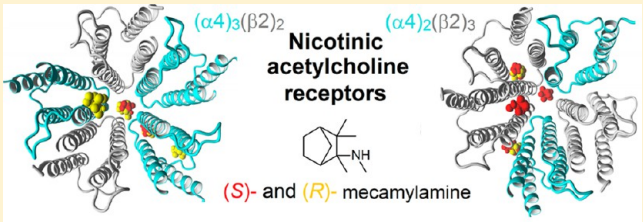

(±)-Mecamylamine hydrochloride (Inversine) was developed for the treatment of hypertension in the 1950s, and its mechanism of action is based on the inhibition of ganglionic nicotinic acetylcholine receptors (AChRs), especially the α3β4 AChR. Because of severe side effects elicited by (±)-mecamylamine (e.g., postural hypotension), and the development of safer drugs for the treatment of hypertension, (±)-mecamylamine was consequently displaced from the market. However, new research on (±)-mecamylamine has demonstrated that this drug possesses anti-addictive, antidepressant, and pro-cognitive activities.[1,2] These new results open the door for the development of (±)-mecamylamine as a therapeutic treatment for several neurological disorders.

(±)-Mecamylamine is the racemic mix of (*S*)-(+)- and (*R*)-(−)-mecamylamine (Figure 1). Electrophysiological results showed that (*S*)-(+)-mecamylamine has inhibitory actions at central human (h) neuronal AChRs superior to those of (*R*)-(−)-mecamylamine, compared to muscle type AChRs.[3] Additional studies determined that (*S*)-(+)-mecamylamine behaves as a positive allosteric modulator (i.e., enhances the activity of an agonist without producing any effect by itself) of the $(\alpha4)_2(\beta2)_3$ stoichiometry (i.e., the so-called highly sensitive α4β2 AChR), whereas (*R*)-(−)-mecamylamine inhibits noncompetitively this receptor stoichiometry, and that (*S*)-(+)-mecamylamine is more effective than (*R*)-(−)-mecamylamine as a noncompetitive inhibitor of the $(\alpha4)_3(\beta2)_2$ stoichiometry (i.e., the so-called weakly sensitive α4β2 AChR).[4] These functional differences correspond very well with the therapeutic effect elicited by each isomer. For example, (*S*)-(+)-mecamylamine was found to be more effective than the (*R*)-(−)-enantiomer in blocking nicotine-induced seizures and produced less suppression of open field locomotor activity than (*R*)-(−)-mecamylamine.[5] On the basis of these and other preclinical results, clinical trials were conducted to determine whether (*S*)-(+)-mecamylamine is an alternative for the treatment of depression.[6]

Received: July 19, 2013
Revised: January 9, 2014
Published: January 17, 2014

dx.doi.org/10.1021/bi400969x | *Biochemistry* 2014, 53, 908−918

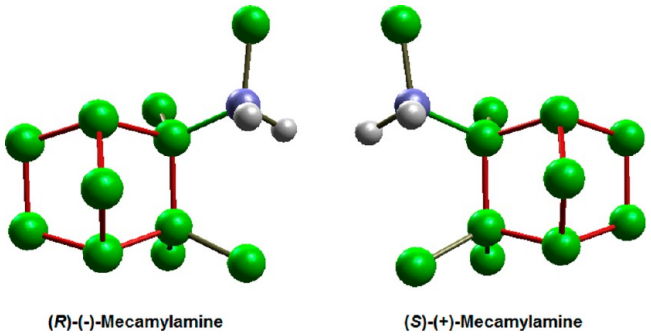

Figure 1. Molecular structures of *exo*-(*S*)-(+)-mecamylamine and *exo*-(*R*)-(−)-mecamylamine in the protonated states. The nitrogen atom is colored blue; hydrogens are colored gray and carbons green. The ligands are shown using the stick mode with aliphatic hydrogen atoms not shown explicitly.

On the basis of the fact that the pharmacological profile of each mecamylamine isomer depends on the $\alpha4\beta2$ AChR stoichiometry,[4] we want to determine whether there are different binding interactions for (*S*)-(+)- and (*R*)-(−)-mecamylamine at each h$\alpha4\beta2$ AChR stoichiometry. In this regard, the transmembrane domain (TMD) of each h$\alpha4$ and h$\beta2$ subunit was first expressed and purified as recently described,[7] and high-resolution nuclear magnetic resonance (NMR) experiments were subsequently performed to determine the direct interaction of each mecamylamine isomer with the respective $(\alpha4)_2(\beta2)_3$- and $(\alpha4)_3(\beta2)_2$-TMD. Additional molecular docking studies were performed to structurally delineate the binding pockets and to determine the molecular orientation of each isomer in the binding pockets. Previous functional and structural studies demonstrated that (±)-mecamylamine partially inhibits the binding of [^{3}H]imipramine to the h$\alpha4\beta2$ and h$\alpha3\beta4$ AChRs.[8,9] However, we do not know if each isomer binds to particular domains at each AChR stoichiometry. Thus, [^{3}H]imipramine competition experiments were performed using h$\alpha4\beta2$ AChR membranes to determine whether each mecamylamine isomer binds to this site.

EXPERIMENTAL PROCEDURES

Materials. [^{3}H]Imipramine (47.5 Ci/mmol) was obtained from PerkinElmer Life Sciences Products, Inc. (Boston, MA) and stored in ethanol at −20 °C. Imipramine hydrochloride, polyethylenimine, leupeptin, bacitracin, pepstatin A, aprotinin, benzamidine, lauryldimethylamine-oxide (LDAO), parmethylsulfonyl fluoride (PMSF), sodium acetate, 2-mercaptoethanol, *N*,*N*-dimethyldodecylamine, and an *N*-oxide solution were purchased from Sigma-Aldrich Co. (St. Louis, MO). Mecamylamine isomers were obtained from Toronto Research Chemicals Inc. (Toronto, ON). (±)-Epibatidine hydrochloride, Geneticin, and hygromycine B were obtained from Tocris Bioscience (Ellisville, MO). κ-Bungarotoxin (κ-BTx) was obtained from Biotoxins Inc. (St. Cloud, FL). Fetal bovine serum (FBS) was obtained from Aleken Biologicals (Nash, TX). Deuterium oxide (D_2O) was obtained from Cambrige Isotope Laboratories, Inc. (Andover, MA). Acetic acid was purchased from Fisher Scientific Co. (Fair Lawn, NJ). Salts were of analytical grade.

Preparation of the Transmembrane Domains (TMDs) of the α4 and β2 Subunits for Solution NMR. The α4- and β2-subunits of the h$\alpha4\beta2$ AChR, with the extracellular and intracellular domains removed by mutagenesis (i.e., α4- and β2-TMD, respectively), were expressed and purified as recently described in detail.[7] Different ratios of α4- and β2-TMDs were prepared for studying interactions of (*S*)-(+)- and (*R*)-(−)-mecamylamine. To avoid strong peak overlap in the NMR spectra, only one ^{15}N-labeled subunit type (α4 or β2) was used in each sample. The isotope-labeled subunit was kept as a dominant component in the mixture to ensure adequate NMR signals from the protein samples. For example, α4 was labeled in $(\alpha4)_3(\beta2)_2$; likewise, β2 was labeled in $(\beta2)_3(\alpha4)_2$. The molar ratios used for $(\alpha4)_3(\beta2)_2$ and $(\alpha4)_2(\beta2)_3$ represent only the sample conditions and by no means represent uniformly assembled pentamers. Another reason to retain the ^{15}N-labeled subunit (^{15}N NMR observable) as a major component and the unlabeled one (invisible in ^{15}N NMR) as the minor component is to keep the total protein concentration below 0.3 mM to prevent protein aggregation. Each sample contains 0.25 mM monomer protein, 1−2% (40−80 mM) LDAO (lauryldimethylamine-oxide) detergent, 10 mM NaCl, 5 mM sodium acetate (pH 4.7), and 20 mM 2-mercaptoethanol to prevent disulfide bond formation. The NMR sample was adjusted to pH 4.7 to prevent signal reduction in ^{1}H−^{15}N TROSY-HSQC NMR spectra due to exchange of backbone amide protons with the solvent; 5% D_2O was added to the samples for deuterium lock in NMR measurements. Each mecamylamine isomer was titrated to the samples using a micropipet, and the mecamylamine concentration in the NMR samples was calculated on the basis of the concentration of the stock solution.

NMR Data Acquisition, Processing, and Analysis. NMR spectra were recorded on a Bruker Avance 900 MHz spectrometer equipped with a triple-resonance inverse-detection cryoprobe (TCI, Bruker Instruments, Billerica, MA) at 45 °C. ^{1}H−^{15}N TROSY-HSQC NMR spectra were recorded for each sample before and after the addition of (*S*)-(+)- or (*R*)-(−)-mecamylamine. The mecamylamine concentrations in the NMR samples were 3, 15, 40, and 100 μM for (*S*)-(+)-mecamylamine and 15, 40, and 100 μM for (*R*)-(−)-mecamylamine. Spectral windows of 13 ppm (1024 data points) in the ^{1}H dimension and 22.5 ppm (104 data points) in the ^{15}N dimension were used, and the relaxation delay was 1.5 s. The ^{1}H chemical shifts were referenced to the DSS resonance at 0 ppm, and the ^{15}N chemical shifts were indirectly referenced.[10] NMR data were processed using NMRPipe version 4.1 and NMRDraw version 1.8[11] and analyzed using Sparky version 3.10.[12] Each processed spectrum had 4096 × 512 data points. The ^{1}H and ^{15}N chemical shift assignments for the α4- and β2-TMD after the addition of mecamylamine were referenced to the previous assignments for the same proteins without drugs.[7] The specific residues involved in the binding of (*S*)-(+)- and (*R*)-(−)-mecamylamine to each α4- and β2-TMD were identified on the basis of drug-induced chemical shift changes in the HSQC spectra.

Molecular Modeling and Docking. The absolute numbering of amino acids varies greatly between subunits; thus, the prime nomenclature (−5′ to 20′) was used. The sequence numbering of the human neuronal α4- and β2-subunits was obtained from the ExPASy Molecular Biology Server (http://www.us.expasy.org).[13] The TMD model of each $(\alpha4)_2(\beta2)_3$ and $(\alpha4)_3(\beta2)_2$ stoichiometry was constructed as recently published.[7]

Each mecamylamine enantiomer (Figure 1), in the protonated and neutral form, was first sketched using HyperChem version 6.03 (HyperCube Inc., Gainesville, FL),

dx.doi.org/10.1021/bi400969x | *Biochemistry* 2014, 53, 908−918

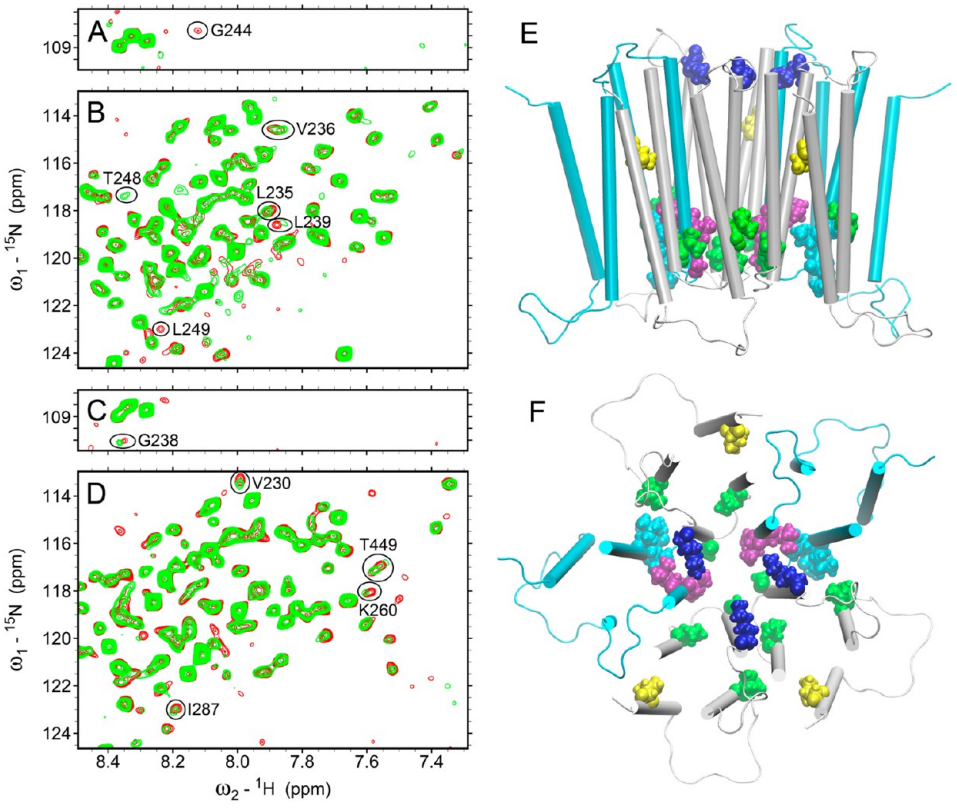

Figure 2. NMR detection of binding of (*S*)-(+)-mecamylamine to the h$\alpha4\beta2$-TMD. Representative regions of ^{1}H−^{15}N TROSY-HSQC NMR spectra of the h$\alpha4\beta2$-TMD in the absence (red) and presence (green) of 15 μM (*S*)-(+)-mecamylamine: (A and B) $(\alpha4)_3(\beta2)_2$-TMD with only the α4-TMD ^{15}N-labeled and visible in the NMR spectra and (C and D) $(\alpha4)_2(\beta2)_3$-TMD with only the β2-TMD ^{15}N-labeled and visible in the NMR spectra. The α4- and β2-TMD residues affected by the drug are labeled with the one-letter amino acid code followed by the sequence number and marked by ovals. (E and F) Side view and top view of the h$\alpha4\beta2$ AChR TMD, respectively. Residues affected by the drug in α4-TMD (cyan) are colored purple (G244, T248, and L249) and cyan (L235, V236, and L239). Residues affected by the drug in β2-TMD (white) are colored green (G238, V230, and I287), blue (K260), and yellow (T449). See Figure S6 of the Supporting Information for the chemical shift changes induced by (*S*)-(+)-mecamylamine as a function of residue number and Figure S8 of the Supporting Information for the chemical shift change or peak intensity decay as a function of drug concentration.

optimized using the semiempirical method AM1 (Polak−Ribiere algorithm to a gradient lower than 0.1 kcal Å^{-1} mol^{-1}), and then transferred for the subsequent step of the ligand docking procedure. Molegro Virtual Docker (MVD 2011.4.3.0, Molegro ApS, Aarhus, Denmark) was used for docking simulations of the flexible molecule into the rigid target of both $(\alpha4)_2(\beta2)_3$- and $(\alpha4)_3(\beta2)_2$-TMD models. To determine the molecular details and orientation of each mecamylamine enantiomer in the domains defined by the NMR results, docking simulations were directed to those domains. The directed molecular dockings were performed using the settings described by Arias et al.,[9,8] including 100 runs, a maximal number of iterations of 10000, and a maximal number of poses of 10.

Preparation of Membranes from HEK293-h$\alpha4\beta2$ Cells. To prepare cell membranes in large quantities, HEK293-h$\alpha4\beta2$ cells were cultured in suspension using nontreated Petri dishes (150 mm × 15 mm) as previously described.[8,9,14] Briefly, cells were cultured in a 1:1 mixture of Dulbecco's modified Eagle's medium containing 3.7 g/L $NaHCO_3$, 1.0 g/L sucrose, stable glutamine (L-alanyl-L-glutamine, 524 mg/L), and Ham's F-12 nutrient mixture (PromoCell GmbH, Heidelberg, Germany) containing 1.176 g/L $NaHCO_3$ supplemented with 10% (v/v) FBS, Geneticin (0.2 mg/mL), and hygromycine B (0.2 mg/mL). After the cells had been cultured at 37 °C, 5% CO_2, and 95% relative humidity for ∼3−4 weeks, they were harvested by being gently scraped and centrifuged at 1000 rpm for 5 min at 4 °C using a Sorvall Super T21 centrifuge. Cells were resuspended in binding saline (BS) buffer [50 mM Tris-HCl, 120 mM NaCl, 5 mM KCl, 2 mM $CaCl_2$, and 1 mM $MgCl_2$ (pH 7.4)] containing 0.025% (w/v) sodium azide and a cocktail of protease inhibitors, including leupeptin, bacitracin, pepstatin A, aprotinin, benzamidine, and PMSF. The suspension was maintained on ice, homogenized using a Polytron PT3000 instrument (Brinkmann Instruments Inc., Westbury, NY), and then centrifuged at 10000 rpm for 30 min at 4 °C. The pellet was finally resuspended in BS buffer containing 20% sucrose (w/v) using the Polytron and briefly (5 × 15 s) sonicated (Branson Ultrasonics Co., Danbury, CT) to ensure maximal homogenization. Cell membranes, containing h$\alpha4\beta2$ AChRs, were frozen at −80 °C until they were required. The total protein was determined using the bicinchoninic acid protein assay (Thermo Fisher Scientific, Rockford, IL).

[^{3}H]Imipramine Competition Binding Experiments Using h$\alpha4\beta2$ AChRs in Different Conformational States. The effect of (*S*)-(+)-mecamylamine was compared to that of (*R*)-(−)-mecamylamine by [^{3}H]imipramine binding to h$\alpha4\beta2$ AChRs in different conformational states using the method previously developed in our laboratory.[8,9] In this regard, AChR membranes (1.5 mg/mL) were suspended in BS buffer with 21

dx.doi.org/10.1021/bi400969x | *Biochemistry* 2014, 53, 908−918

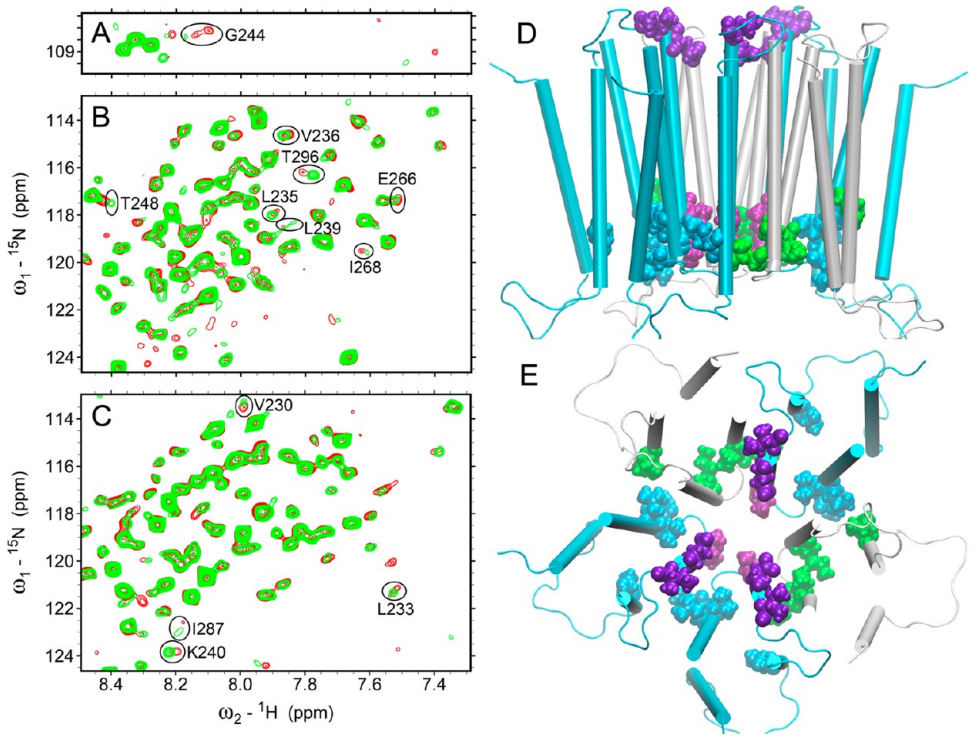

Figure 3. NMR detection of binding of (*R*)-(−)-mecamylamine to the hα4β2-TMD. Representative regions of $^{1}H-^{15}N$ TROSY-HSQC NMR spectra of the hα4β2-TMD in the absence (red) and presence (green) of 15 μM (*R*)-(−)-mecamylamine: (A and B) $(\alpha4)_3(\beta2)_2$-TMD with only the α4-TMD ^{15}N-labeled and visible in the NMR spectra and (C) $(\alpha4)_2(\beta2)_3$-TMD with only the β2-TMD ^{15}N-labeled and visible in the NMR spectra. The α4- and β2-TMD residues affected by the drug are labeled with the one-letter amino acid code followed by the sequence number and marked by ovals. (D and E) Side view and top view of the hα4β2 AChR TMD, respectively. Residues affected by the drug in α4-TMD (cyan) are colored purple (G244 and T248), cyan (L235, V236, L239, and T296), and violet (E266 and I268). Residues affected by the drug in β2-TMD (white) are colored green (V230, L233, K240, and I287). See Figure S7 of the Supporting Information for the chemical shift changes induced by (*R*)-(−)-mecamylamine as a function of residue number and Figure S9 of the Supporting Information for the chemical shift change or peak intensity decay as a function of drug concentration.

nM [^{3}H]imipramine in the presence of 0.1 μM κ-BTx (resting/κ-BTx-bound state) or 0.1 μM (±)-epibatidine (desensitized/epibatidine-bound state) and preincubated for 30 min at room temperature (RT). Bungarotoxins such as κ-BTx are competitive antagonists that maintain the AChRs in the resting (closed) state.[15] The nonspecific binding was assessed in the presence of 100 μM imipramine. The total volume was divided into aliquots, and increasing concentrations of (*S*)-(+)- or (*R*)-(−)-mecamylamine were added to each tube and incubated for 90 min at RT. AChR-bound [^{3}H]imipramine was then separated from free ligand by a filtration assay using a 48-sample harvester system with GF/B Whatman filters (Brandel Inc., Gaithersburg, MD), previously soaked with 0.5% polyethylenimine for 30 min. The membrane-containing filters were transferred to scintillation vials with 3 mL of Bio-Safe II (Research Product International Corp., Mount Prospect, IL), and the radioactivity was determined using a Beckman LS6500 scintillation counter (Beckman Coulter, Inc., Fullerton, CA).

The concentration−response data were curve-fitted by nonlinear least-squares analysis using Prism (GraphPad Software, San Diego, CA). The observed IC_{50} values from the competition experiments described above were transformed into inhibition constant (K_i) values using the Cheng−Prusoff relationship:[16]

$$K_i = IC_{50}/(1 + [[^{3}H]\text{imipramine}]/K_d^{\text{imipramine}}) \quad (1)$$

where [[^{3}H]imipramine] is the initial concentration of [^{3}H]imipramine and $K_d^{\text{imipramine}}$ is the [^{3}H]imipramine dissociation constant for the hα4β2 AChR (0.83 μM).[8] The K_i and n_H values were summarized in Table 2.

RESULTS

Interaction of (*S*)-(+)- and (*R*)-(−)-Mecamylamine with the α4β2-TMDs Determined by NMR. The interaction of (*S*)-(+)- and (*R*)-(−)-mecamylamine with specific residues from the $(\alpha4)_3(\beta2)_2$- and $(\alpha4)_2(\beta2)_3$-TMDs was assessed by measuring the change in the peak chemical shift or peak intensity from the of $^{1}H-^{15}N$ TROSY-HSQC spectra after addition of the drug. The α4β2-TMDs form pentameric assemblies under the NMR experimental condition (Figure S1 of the Supporting Information). Figures 2 and 3 show representative regions of the $(\alpha4)_3(\beta2)_2$- and $(\alpha4)_2(\beta2)_3$-TMD TROSY-HSQC spectra in the absence and presence of (*S*)-(+)- and (*R*)-(−)-mecamylamine, respectively. Several residues demonstrated significant chemical shift changes resulting from drug interaction, suggesting that each isomer interacts with the protein only at a few specific locations in the AChR TMD. The effects of the drug on all assigned residues of the $(\alpha4)_3(\beta2)_2$- and $(\alpha4)_2(\beta2)_3$-TMDs are shown in Figures S2−S9 of the Supporting Information.

The hα4β2-TMD residues showing significant chemical shifts by (*S*)-(+)-mecamylamine include those at TM1 (i.e., α4-Leu235, α4-Val236, α4-Leu239, and β2-Val230), TM2 (i.e., β2-Gly238 and β2-Lys260), TM3 (i.e., β2-Ile287), and TM4 (i.e., β2-Thr449), with α4-Leu239 and β2-Val230 being the most sensitive to the drug (Figure 2). In addition, the peak

dx.doi.org/10.1021/bi400969x | *Biochemistry* 2014, 53, 908−918

Table 1. Emulated Binding Energies (MolDock Score) for Each Mecamylamine Enantiomer, in the Protonated and Neutral State, Interacting with Luminal (L) and Nonluminal Sites at Different h$\alpha4\beta2$-TMD Stoichiometries

Enantiomer	AChR TMD stoichiometry	Binding site location	TM1	TM2	TM3	MolDock Score (kJ/mol) (neutral/protonated state)
(*S*)-(+)-mecamylamine	$(\alpha4)_2(\beta2)_3$	L1		$\beta2$-G238 $(-3')^{a,b}$		−60/−79
				$\alpha4$-G244 $(-3')^{a,b}$		
				$\alpha4$-E242 $(-5')^{b}$		
		L2		$\beta2$-K260 $(20')^{a,b}$		−38/−35
				$\beta2$-L256 $(16')^{b}$		
		$\alpha4/\beta2$-intersubunit	$\alpha4$-L235^{a,b}		$\beta2$-I287^{a,b}	−28/−24
			$\alpha4$-Y238^{b}		$\beta2$-V291^{b}	
		$\beta2$-intersubunit	$\beta2$-V230^{a,b}	$\beta2$-L243 $(3')^{b}$	$\beta2$-S290^{b}	−30/−28
			$\beta2$-L233^{b}	$\beta2$-K240 $(-1')^{b}$		
	$(\alpha4)_3(\beta2)_2$	L1′[c]		$\alpha4$-T248 $(2')^{a,b}$		−32/−53
				$\beta2$-G238 $(-3')^{a,b}$		
		$\alpha4$-intrasubunit	$\alpha4$-L235^{a}	$\alpha4$-L249 $(3')^{a}$		−40/−45
			$\alpha4$-V236^{a,b}			
			$\alpha4$-L239^{a}	$\alpha4$-K246 $(-1')^{b}$		
			$\alpha4$-P240^{b}			
(*R*)-(−)-mecamylamine	$(\alpha4)_2(\beta2)_3$	$\alpha4/\beta2$-intersubunit	$\alpha4$-L235^{a,b}		$\beta2$-I287^{a,b}	−25/−27
			$\alpha4$-Y238^{b}		$\beta2$-V291^{b}	
		$\beta2$-intersubunit	$\beta2$-V230^{a,b}	$\beta2$-L243 $(3')^{b}$	$\beta2$-S290^{b}	−31/−27
			$\beta2$-L233^{a,b}	$\beta2$-K240 $(-1')^{a,b}$		
	$(\alpha4)_3(\beta2)_2$	L1′[c]		$\alpha4$-T248 $(2')^{a,b}$		−34/−51
				$\alpha4$-G244 $(-3')^{a}$		
				$\beta2$-G238 $(-3')^{b}$		
		L2′[c]		$\alpha4$-E266 $(20')^{a,b}$		−24/−28
				$\alpha4$-I267 $(21')^{b}$		
				$\alpha4$-I268 $(22')^{a}$		
		$\alpha4$-intrasubunit	$\alpha4$-L235^{a}	$\alpha4$-K246 $(-1')^{b}$		−48/−51
			$\alpha4$-V236^{a,b}			
			$\alpha4$-L239^{a}			
			$\alpha4$-P240^{b}			
		$\alpha4$-TM3-intrasubunit			$\alpha4$-T296^{a,b}	−36/−37
					$\alpha4$-I295^{b}	
					$\alpha4$-V298^{b}	

Numbers in parentheses indicate the positions of the residues along the TM2, where locations 20′, 2′, −2′, and −5′ are considered the extracellular (or outer), threonine, intermediate, and cytoplasmic (or inner) amino acid rings, respectively.

[a]Residues involved in binding based on the NMR [b]Molecular docking results [c]Different orientations of the ligand in partially overlapping sites

intensity of $\alpha4$-Thr248 (at TM2) increased significantly, whereas the peak intensity of $\alpha4$-Gly244 and $\alpha4$-Leu249 (at TM2) decreased significantly. A preliminary assumption is that residues $\beta2$-Lys260, $\alpha4$-Gly244, $\alpha4$-Thr248, and $\beta2$-Gly238, which are facing the ion channel lumen, are part of luminal (L) binding sites (see Table 1). Residues $\alpha4$-Leu235, $\alpha4$-Val236, $\alpha4$-Leu239, $\beta2$-Val230, and $\beta2$-Ile287, which are located at the cytoplasmic end of the respective TMDs, as well as $\alpha4$-Leu249, which is facing TM1, might be forming different nonluminal sites (see Table 1).

The interaction of (*R*)-(−)-mecamylamine with the $\alpha4\beta2$-TMD is shown in Figure 3 and Figures S3 and S4 of the Supporting Information. The residues involved in drug binding are located at TM1 (i.e., $\alpha4$-Leu235, $\alpha4$-Val236, $\alpha4$-Leu239, $\beta2$-Val230, and $\beta2$-Leu233), TM2 (i.e., $\alpha4$-Glu266, $\alpha4$-Ile268, and $\beta2$-Lys240), and TM3 (i.e., $\alpha4$-Thr296 and $\beta2$-Ile287) (Figure 3). The chemical shifts of $\alpha4$-Leu239, $\alpha4$-Thr296, and $\beta2$-Val230 were the most affected by this enantiomer. We also observed significant intensity changes for $\alpha4$-Gly244 and $\alpha4$-Thr248 located at TM2. These residues may be forming an L site close to the threonine ring (position 2′). In contrast to the results with (*S*)-(+)-mecamylamine, (*R*)-(−)-mecamylamine affected $\alpha4$-Glu266 more than it affected $\beta2$-Lys260. Thus, (*R*)-(−)-mecamylamine may be interacting with an L binding site formed by $\alpha4$-Glu266 and $\alpha4$-Ile268 (Figure 3B), which are located close to the extracellular mouth of the ion channel. In general, (*R*)-(−)-mecamylamine binds to the same NL sites described for (*S*)-(+)-mecamylamine (Table 1). However, the large chemical shift observed at $\alpha4$-Thr296 (at TM3) (Figure 3B) in addition to the effect on $\beta2$-Leu233 (at TM1) (Figure 3C) supports the existence of additional NL sites for (*R*)-(−)-mecamylamine (Table 1).

Molecular Docking. Each mecamylamine enantiomer was directed to be docked to the various pockets formed by the residues interacting with mecamylamine previously determined by the NMR experiments (Figures 4 and 5). Because mecamylamine is ∼100% in the protonated form at physiological pH,[8,9] the different poses are shown in the protonated state. Nevertheless, the same poses were observed for the neutral form. The results from the directed docking of (*S*)-(+)- and (*R*)-(−)-mecamylamine at the $(\alpha4)_2(\beta2)_3$- and $(\alpha4)_3(\beta2)_2$-TMD stoichiometries indicate that each enantiomer presents different modes of interaction at several L and NL binding sites (see Table 1). The first docking sphere includes

dx.doi.org/10.1021/bi400969x | *Biochemistry* 2014, 53, 908−918

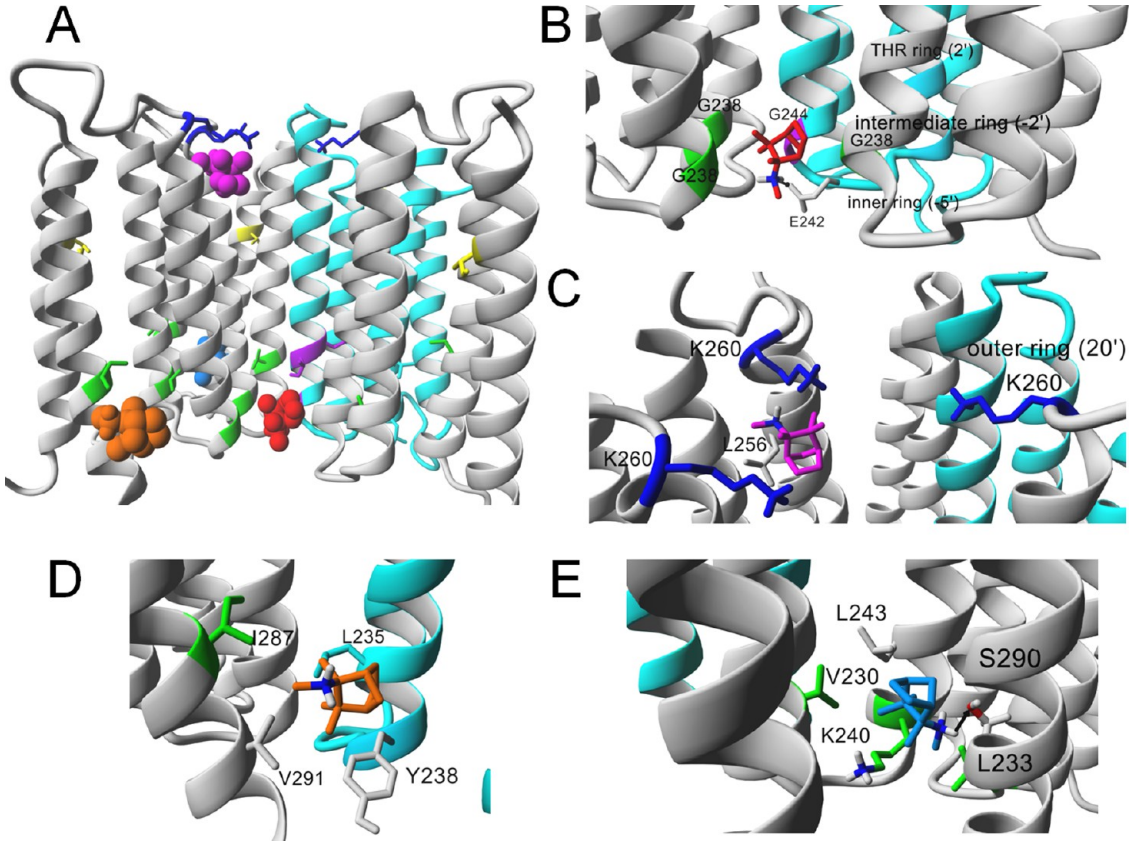

Figure 4. Docking site locations for protonated (*S*)-(+)-mecamylamine in the $(\alpha4)_2(\beta2)_3$-TMD model. (A) Side view of the luminal (L) and nonluminal (i.e., $\alpha4/\beta2$- and $\beta2$-intersubunit) binding sites for (*S*)-(+)-mecamylamine. The L binding sites comprise residues near the cytoplasmic (L1 in red) and extracellular (L2 in magenta) ion channel mouths. The nonluminal binding sites are located at the boundary of TM3 and TM1 near the cytoplasmic portions of the respective $\beta2$- and $\alpha4$-subunits (i.e., $\alpha4/\beta2$-intersubunit site colored orange) and between two $\beta2$-TMDs (i.e., $\beta2$-intersubunit site colored light blue). (B) Detailed view of L1 (red). (*S*)-(+)-Mecamylamine interacts by van der Waals contacts with the $\beta2$-Gly238 and $\alpha4$-Gly244 backbones (position −3′). The black arrow indicates the short-range (distance of <4.5 Å) electrostatic interaction between the positively charged amino group of (*S*)-(+)-mecamylamine and the carboxylic group of $\alpha4$-Glu242 at the cytoplasmic or inner ring (position −5). (C) Detailed view of L2 (magenta). The methyl moiety of (*S*)-(+)-mecamylamine interacts with the aliphatic portion of $\beta2$-Lys260 at the outer ring (position 20′), whereas its positively charged amino group is oriented toward the $\beta2$-Leu256 backbone (position 16′). (D) Detailed view of the $\alpha4/\beta2$-intersubunit site (orange). (*S*)-(+)-Mecamylamine is oriented predominantly toward $\alpha4$-Leu235 (at TM1) but also interacts by van der Waals contacts with nonpolar residues, including $\beta2$-Tyr238, $\beta2$-Ile287, and $\beta2$-Val291 (at TM3). (E) Detailed view of the $\beta2$-intersubunit site (light blue). (*S*)-(+)-Mecamylamine binds by van der Waals interactions to nonpolar residues at TM1 (i.e., Val230 at one $\beta2$-subunit and Leu233 at a different $\beta2$-subunit) and TM2 (i.e., $\beta2$-Leu243, which is not facing the ion channel lumen), and with the nonpolar portion of $\beta2$-Lys240 (position −1′). In addition, the amino moiety of the ligand forms a hydrogen bond with the hydroxyl group of $\beta2$-Ser290 (at TM3). In panels A–E, for the sake of clarity, the $\alpha4$-subunits are colored cyan and the $\beta2$-subunits white. Oxygen atoms are colored red, nitrogens blue, and hydrogens white. In panels A–C, for the sake of clarity, one $\alpha4$-subunit is hidden; thus, the order of explicitly shown subunits is $\beta2$, $\beta2$, $\alpha4$, and $\beta2$ (from left to right, respectively). The ligands are rendered in ball (A) or stick (B–E) mode, whereas the residues are shown explicitly in stick mode. All nonpolar hydrogen atoms are hidden. Residues determined by NMR experiments are colored as in Figure 2E, F.

residues $\alpha4$-Gly244 and $\beta2$-Gly238, which the NMR experiments indicated were important (Table 1). With regard to the $(\alpha4)_2(\beta2)_3$-TMD stoichiometry, the docking results indicate that the most favorable energy of binding was obtained for (*S*)-(+)-mecamylamine interacting with L1 (Table 1), which is located at the cytoplasmic mouth of the ion channel (Figure 4A). In this site, the nonpolar portion of (*S*)-(+)-mecamylamine interacts with the $\beta2$-Gly238 and $\alpha4$-Gly244 backbones (position −3′) by van der Waals contacts, whereas its positively charged amino group forms a short-range (distance of <4.5 Å) electrostatic interaction with the carboxylic group of $\alpha4$-Glu242 (position −5′) at the cytoplasmic or inner ring (Figure 4B). Interestingly, in the case of the $(\alpha4)_3(\beta2)_2$-TMD stoichiometry, (*S*)-(+)- and (*R*)-(−)-mecamylamine also present favorable energies of binding at this site (Table 1). Each isomer maintains its interaction with $\beta2$-Gly238, while the nitrogen from the ligand's amino group forms a hydrogen bond with the hydroxyl group of $\alpha4$-Thr248, which the NMR results indicated was important (Table 1). Although these poses include $\alpha4$-Thr248 at the threonine ring (position 2′) (not shown) and (*S*)-(+)-mecamylamine has a different orientation with respect to that found in the $(\alpha4)_2(\beta2)_3$-TMD model (see Figure 4B), it is considered a homologous site (partially overlapping) with respect to L1, and thus, it is named L1′ (compare L1 and L1′ in Table 1).

The second docking sphere includes residue $\beta2$-Lys260, which the NMR experiments indicated was important (Figure 2C and Table 1). The docking results at the $(\alpha4)_2(\beta2)_3$-TMD stoichiometry indicate that (*S*)-(+)-mecamylamine interacts with this site with a favorable energy of binding (see L2 in Table 1). L2 is located close to the extracellular mouth of the ion channel (Figure 4A), where the methyl moiety of (*S*)-

dx.doi.org/10.1021/bi400969x | *Biochemistry* 2014, 53, 908–918

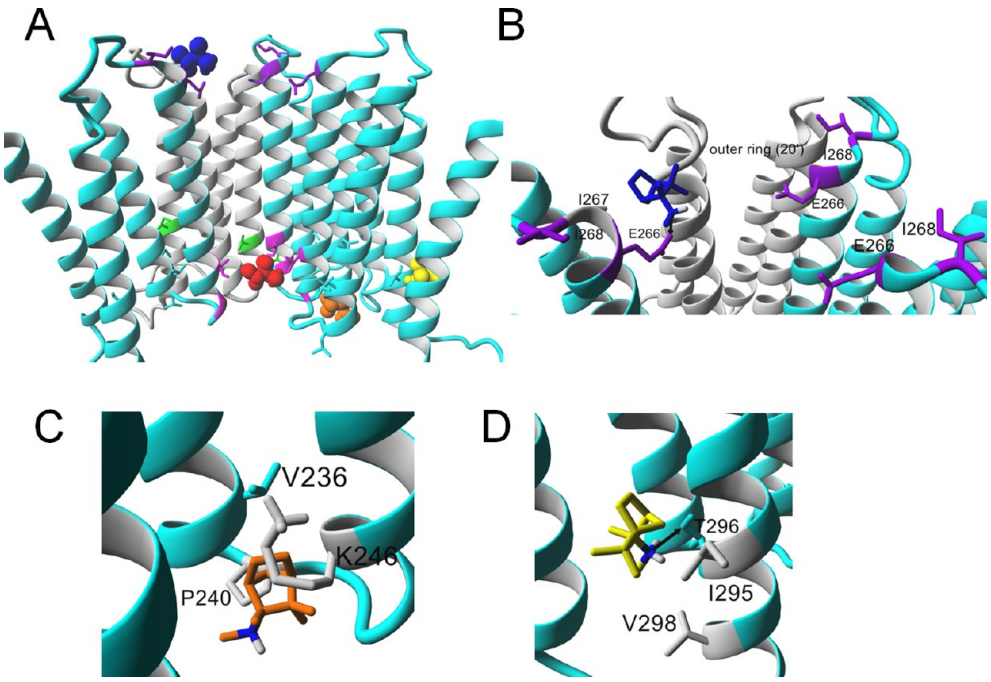

Figure 5. Docking site location for protonated (*R*)-(−)-mecamylamine in the $(\alpha4)_3(\beta2)_2$-TMD model. (A) Side view of the binding sites for (*R*)-(−)-mecamylamine. The molecule interacts with two luminal sites, one close to the threonine (THR) ring (position 2′) (L1′ colored red) and another close to the extracellular ring (position 20′) (L2′ colored blue), as well as with two nonluminal binding sites [i.e., the α4-intrasubunit (orange) and α4-TM3-intrasubunit (yellow) sites]. Because the location of L1′ is similar to that found for (*S*)-(+)-mecamylamine in the $(\alpha4)_3(\beta2)_2$-TMD model (see L1 in Figure 4B), the molecular details are not shown. (B) Detailed view of L2′ (blue). The positively charged amino group of (*R*)-(−)-mecamylamine forms a short-range (distance of <4.5 Å) electrostatic interaction with the carboxylic group of α4-Glu266 (position 20′), whereas the aliphatic portion of the molecule binds to α4-Ile267 (position 21′) by van der Waals interactions. Although the orientation of (*R*)-(−)-mecamylamine is different from that of (*S*)-(+)-mecamylamine (see Figure 4C), it binds to a homologous site in the $(\alpha4)_2(\beta2)_3$-TMD model. (C) Detailed view of the α4-intrasubunit site (orange). (*R*)-(−)-Mecamylamine interacts by van der Waals contacts with the aliphatic portion of α4-Lys246 (at TM2 but not facing the ion channel lumen), and with nonpolar residues α4-Pro240 and α4-Val236 (at TM1). (D) Detailed view of the α4-TM3-intrasubunit site (yellow). The black arrow indicates the hydrogen bond between the amino moiety of (*R*)-(−)-mecamylamine and the hydroxyl group of α4-Thr296 (at TM3). In addition, the aliphatic portion of the molecule interacts by van der Waals contacts with nonpolar residues α4-Ile295 and α4-Val298 (at TM3). Residues determined by NMR experiments are colored as in Figure 3D, E. Additional details are given in the legend of Figure 4.

(+)-mecamylamine binds by van der Waals interactions to the aliphatic portion of β2-Lys260 located at the outer ring (position 20′), whereas its positively charged amino group is oriented toward the β2-Leu256 backbone (position 16′) (Figure 4C). Interestingly, (*R*)-(−)-mecamylamine binds to a homologous site in the $(\alpha4)_3(\beta2)_2$-TMD stoichiometry (Figure 5B). In this energetically less favorable orientation (Table 1), the positively charged amino group of the isomer forms a short-range electrostatic interaction with the carboxylic group of α4-Glu266 (position 20′), whereas its aliphatic portion interacts by van der Waals contacts with the aliphatic moiety of α4-Ile267 (position 21′) (Figure 5B). α4-Glu266 is identified as an important residue by the NMR experiments (Figure 3A and Table 1).

The third docking sphere includes α4-Leu235, α4-L239, and β2-Ile287, which the NMR experiments for each enantiomer indicated were residues (Figures 2A,C and 3A,C and Table 1). The docking results indicate that (*S*)-(+)-mecamylamine interacts with comparatively less energy of binding with the intersubunit site located between the α4- and β2-TMDs (see the α4/β2-intersubunit site in Table 1). In this site, (*S*)-(+)-mecamylamine interacts by van der Waals contacts with residues located at TM3 (i.e., β2-Ile287 and β2-Val291) and TM1 (i.e., α4-Leu235 and α4-Tyr238) (Figure 4D). Because the pose for (*R*)-(−)-mecamylamine at this site is structurally and energetically similar to that for (*S*)-(+)-mecamylamine (see Table 1), the model is not shown.

The fourth docking sphere includes residue β2-Thr449 (at TM4), which was significantly affected by (*S*)-(+)-mecamylamine during the NMR experiments (Figure 2C). Because the docking results indicate that this interaction is relatively less favorable (−4 and −8 kJ/mol for the protonated and neutral states, respectively), this site is not included.

The last docking sphere includes residues β2-Val230, β2-Leu233, and β2-Lys240, which the NMR experiments indicated were important (Table 1 and Figures 2C and 3B). The docking results indicate that the interaction of (*S*)-(+)-mecamylamine (Figure 4E) and (*R*)-(−)-mecamylamine (not shown) at the interface of two β2 subunits is energetically favorable (see the β2-intersubunit site in Table 1). Each ligand interacts by van der Waals contacts with nonpolar residues TM1 Val230 and TM2 Leu243 from one β2-subunit and with TM1 Leu233 from a different β2-subunit; the methyl moiety from its amino group interacts by van der Waals contacts with the aliphatic portion of β2-Lys240 (at TM1), and its amino moiety forms a hydrogen bond with the hydroxyl group of β2-Ser290 (Figure 4E).

One of the used docking spheres of the $(\alpha4)_3(\beta2)_2$-TMD model includes α4-Leu235, α4-Leu239, α4-Val236, and α4-Leu249, considered to be important residues by the NMR results (see Table 1). The docking results show that both (*S*)-

dx.doi.org/10.1021/bi400969x | *Biochemistry* 2014, 53, 908−918

(+)-mecamylamine (not shown) and (*R*)-(−)-mecamylamine (Figure 5C) interact within the α4-TMD with similar binding energies (see the α4-intrasubunit site in Table 1). Each isomer interacts by van der Waals contacts with the aliphatic portions of α4-Lys246 (at TM2 but not facing the ion channel lumen) and α4-Val236 (at TM1) as well as with nonpolar residue α4-Pro240 (at TM1). However, the enantiomers do not interact with α4-Leu235, which was found at the α4/β2-intersubunit site (Figure 4D).

The last docking sphere at the $(\alpha4)_3(\beta2)_2$-TMD stoichiometry includes α4-Thr296, considered to be important by the NMR experiments (Figure 3A). The docking results show that (*R*)-(−)-mecamylamine interacts with the α4-TM3-intrasubunit site with a favorable energy of binding (Table 1). More specifically, a hydrogen bond is formed between the nitrogen atom of the amine moiety of the enantiomer and the hydroxyl group of α4-Thr296 (at TM3), and van der Waals interactions are observed with the nonpolar portion of α4-Ile295 and α4-Val298 (also located at TM3) (Figure 5D).

[^{3}H]Imipramine Competition Binding. (±)-Mecamylamine partially inhibits binding of [^{3}H]imipramine to hα4β2 AChRs.[7] However, we do not know the binding affinity of each enantiomer, which could be important for explaining the distinct pharmacologic activity of (*S*)-(+)- and (*R*)-(−)-mecamylamine on each α4β2 AChR stoichiometry.[4] In this regard, the effect of each enantiomer on the binding of [^{3}H]-imipramine to hα4β2 AChRs in the resting (κ-BTx-bound) and desensitized (epibatidine-bound) states was determined (Figure 6). The apparent K_i values suggest that both enantiomers practically do not bind to the [^{3}H]imipramine binding site at hα4β2 AChRs in either the resting (>150 μM) or desensitized (>220 μM) state (Table 2). The observed n_H values are lower than unity (~0.5) (see Table 2), indicating a negative cooperative interaction between imipramine and each mecamylamine isomer. In turn, this suggests that both mecamylamine enantiomers do not overlap the imipramine sites at the hα4β2 AChR.

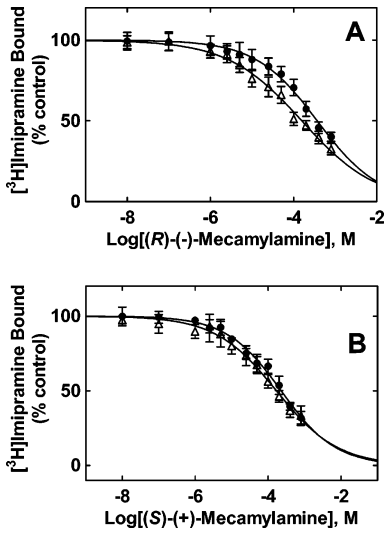

Figure 6. Inhibition of binding of [^{3}H]imipramine to hα4β2 AChRs by (*R*)-(−)-mecamylamine (A) or (*S*)-(+)-mecamylamine (B) in different conformational states. hα4β2 AChR membranes (1.5 mg/mL) were equilibrated (90 min) with 21 nM [^{3}H]imipramine, in the presence of 0.1 μM κ-BTx (resting state) (△) or 1 μM (±)-epibatidine (desensitized state) (●) and increasing concentrations of (A) (*R*)-(−)-mecamylamine or (B) (*S*)-(+)-mecamylamine. Each plot is the combination of two or three separate experiments each performed in triplicate. From these plots, the IC_{50} and n_H values were obtained by nonlinear least-squares fit, and the apparent K_i values were calculated using eq 1 and are summarized in Table 1.

DISCUSSION

This study is an attempt to determine, at the molecular level, how each mecamylamine enantiomer interacts with particular regions from the $(\alpha4)_2(\beta2)_3$- and $(\alpha4)_3(\beta2)_2$-TMDs. In this regard, high-resolution NMR, molecular docking, and radioligand binding approaches were applied.

The NMR experiments determined the interaction of each mecamylamine enantiomer with residues from the respective $(\alpha4)_2(\beta2)_3$- and $(\alpha4)_3(\beta2)_2$-TMD stoichiometries. The high-quality NMR spectra showed what different residues from the α4- and β2-TMDs are significantly affected by both enantiomers (Figures 2 and 3). The results indicate that although the interactions of both enantiomers are similar, some differences are observed. For instance, (*S*)-(+)-mecamylamine interacts with β2-Lys260 at L2 (located at the outer ring, position 20′), whereas the (*R*)-(−)-enantiomer prefers α4-Glu266 at the same position. Because mecamylamine has a pK_a of 11.2,[17] it will be protonated either at pH 4.7 (i.e., used in our NMR experiments) or at physiological pH. However, α4-Glu266, which is charged at physiological pH (pK_a = 4.2), can be partially neutralized at pH 4.7. In this regard, the electrostatic interaction between protonated mecamylamine and α4-Glu266 would be stronger at physiological pH than at the experimental pH.

The NMR results first discriminated the residues involved in the binding of each mecamylamine enantiomer at the α4β2-TMD. These residues were subsequently tested by using different docking spheres. The docking experiments determined the mode of binding and the molecular orientation of each enantiomer in the L and NL binding sites at both TMD stoichiometries. Each enantiomer, in the protonated and neutral state, interacts with binding domains by a combination of van der Waals, hydrogen bond, and electrostatic contacts. In addition to residues identified by NMR, docking simulations suggested that additional residues may possibly be involved in ligand binding.

With regard to the luminal sites, (*S*)-(+)- and (*R*)-(−)-mecamylamine bind with slightly different orientations at sites located close to the cytoplasmic (compare L1 vs L1′) and extracellular (compare L2 vs L2′) mouths of the hα4β2-TMD. Although a mecamylamine binding site was previously located near the extracellular mouth of the hα4β2 and hα3β4 AChR ion channels[8,9] coincident with the L2/L2′ site, recent results from our laboratory indicate that mecamylamine enantiomers may interact with a luminal site located in the middle of the *Torpedo* AChR ion channel, as well.[18] This divergence suggests that different AChR subtypes may have distinct binding site locations for mecamylamine enantiomers. A binding domain close to the extracellular mouth was also characterized for serotonin selective reuptake inhibitors[19] at neuronal AChRs, as well as for SADU-3-72 (a bupropion photoactivatable analogue)[20] and other NCAs[21] at muscle AChRs. Previous photoaffinity labeling data indicate that PCP may bind to the threonine ring (position 2′) from *Torpedo* AChRs, which is closer to the cytoplasmic mouth[22] (overlapping the L1/L1′ site). On the basis of our previously published data,[8] and the radioligand (Table 2) and docking (Table 1) results presented

dx.doi.org/10.1021/bi400969x | *Biochemistry* 2014, 53, 908−918

Table 2. Apparent Binding Affinities of Mecamylamine Enantiomers for the [^{3}H]Imipramine Site(s) at the h$\alpha4\beta2$ AChR

	resting/κ-BTx-bound state[a]		desensitized/epibatidine-bound state[b]	
enantiomer	apparent K_i (μM)	n_H[c]	apparent K_i (μM)	n_H[c]
(*R*)-(−)-mecamylamine	154 ± 23	0.49 ± 0.04	360 ± 59	0.58 ± 0.07
(*S*)-(+)-mecamylamine	203 ± 35	0.58 ± 0.07	223 ± 32	0.58 ± 0.05

[a]The apparent K_i values for the mecamylamine isomers were obtained in the presence of 0.1 μM κ-BTx from Figure 6, according to eq 1. [b]The apparent K_i values for the mecamylamine isomers were obtained in the presence of 0.1 μM (±)-epibatidine from Figure 6, according to eq 1. [c]Hill coefficients.

here, we can infer that each mecamylamine enantiomer does not directly bind to the imipramine luminal site, located in the middle of the h$\alpha4\beta2$ AChR ion channel. Nevertheless, we are conducting new docking experiments to demonstrate whether imipramine has additional NL sites that may coincide with mecamylamine enantiomers and other NCAs.

With regard to the NL sites, there are some similarities between both enantiomers interacting with the $\alpha4/\beta2$-intersubunit (i.e., cytoplasmic end of $\alpha4$-TM1 and $\beta2$-TM3) and $\beta2$-intersubunit (i.e., cytoplasmic end of two $\beta2$-TMDs) sites at the $(\alpha4)_2(\beta2)_3$-TMD, as well as with the $\alpha4$-intersubunit (i.e., at the cytoplasmic ends of $\alpha4$-TM1 and $\alpha4$-TM2) at the $(\alpha4)_3(\beta2)_2$-TMD. An important distinction between the enantiomers is that (*R*)-(−)-mecamylamine binds to the $\alpha4$-TM3-intrasubunit site that is not found for (*S*)-(+)-mecamylamine. Aside from this difference, the existence of NL sites might be related to the trapping blocking mechanism previously described for (±)-mecamylamine by Giniatullin and colleagues.[23] After agonist-induced activation, (±)-mecamylamine penetrates and blocks open AChR channels in a voltage-dependent manner; shortly after channel closure, the molecule reaches the NL site(s), remaining trapped in a less ionic environment, which supports the voltage independence of the trapping mechanism.[23]

New results for *Torpedo* AChRs indicate that mecamylamine enantiomers interact with several NL binding sites.[17] One of them, the intersubunit site, includes γ-Val297, which corresponds to $\beta2$-Ile287 at the $\alpha4/\beta2$-intersubunit site observed for both mecamylamine enantiomers at the $(\alpha4)_2(\beta2)_3$-TMD (Table 1). Interestingly, several mecamylamine binding sites coincide with the anesthetic binding domains found in the proton-activated ion channel from the bacterium *Erwinia chrysanthemi* (i.e., ELIC)[24] and in the $\alpha4\beta2$-TMD.[25] More precisely, halothane overlaps several binding domains found for mecamylamine enantiomers in the $\alpha4\beta2$-TMD, including residues $\alpha4$-Val236, $\alpha4$-Leu239, and $\alpha4$-Leu249 (at the $\alpha4$-intrasubunit site), $\beta2$-Leu233 (at the $\beta2$-intersubunit site), $\beta2$-Lys260 (at L2), and $\alpha4$-Ile268 (at L2′).[25] In addition to the L2′ (i.e., $\alpha4$-Ile268) and $\alpha4$-intrasubunit (i.e., $\alpha4$-Lys246) sites, ketamine overlaps $\beta2$-Ile287 (at the $\alpha4/\beta2$-intersubunit site). In the case of ELIC, the intersubunit site closer to the cytoplasmic end of the TMD overlaps the $\alpha4/\beta2$-intersubunit site presented in this work. In particular, the bromo form interacts with M3-Ile278, M3-Ile282, and M1-Trp225, corresponding to the residues (i.e., $\beta2$-Ile287, $\beta2$-Val291, and $\alpha4$-Tyr238, respectively) in contact with either mecamylamine enantiomer at the $(\alpha4)_2(\beta2)_3$-TMD (Table 1).

Many different rearrangements in the conformation of the AChR have been proposed to be responsible for channel opening after agonist activation. One of them states that the rotation of the M2 segments around their helix axis is important for channel gating,[26−28] whereas others argue that the switching of the hydrophobic residues located along the closed ion channel (especially between positions 9′ and 17′) to polar residues in the open state is important for channel conductivity.[29,30] On the basis of these two models, we hypothesized that binding of mecamylamine to the NL sites may impede the rotation of the M2 segments, disrupting the hydrophobic to polar residue switching, finally maintaining the receptor in a nonconducting conformation.

Previous results indicated that (*S*)-(+)-mecamylamine is more effective than the (*R*)-(−)-mecamylamine in inhibiting $(\alpha4)_3(\beta2)_2$ AChRs, and that it also potentiates the agonist-induced activation of $(\alpha4)_2(\beta2)_3$ AChRs.[4] The observed differences in binding site locations may explain the distinct pharmacologic activity of each isomer at each stoichiometry. For example, on the basis of the NMR and docking studies, we found that (*R*)-(−)-mecamylamine binds to the $\alpha4$-TM3-intrasubunit site at the $(\alpha4)_3(\beta2)_2$-TMD that is not found for (*S*)-(+)-mecamylamine. In this regard, this site may be related to the inhibitory activity mediated by (*R*)-(−)-mecamylamine on the $(\alpha4)_3(\beta2)_2$ AChR.[4]

On the basis of our NMR studies, pentameric assemblies of $\alpha4\beta2$-TMDs undergo substantial dynamics. The same feature has also been observed in the human $\alpha1$ glycine[31] and human $\alpha7$ TMDs.[32] The intrinsic motion of the pentameric $\alpha4\beta2$-TMD structure may contribute to the relatively small chemical shift changes upon drug binding.

Our findings provide the first insight into the direct molecular interactions between the mecamylamine enantiomers and the h$\alpha4\beta2$-TMD stoichiometries. The application of several approaches allowed us to characterize different L and NL binding sites for each mecamylamine enantiomer. These findings are valuable for the understanding of the allosteric modulation elicited by each enantiomer, and this basic knowledge could be beneficial for the development of novel therapies for the treatment of several neurological disorders involving $\alpha4\beta2$ AChRs.

■ ASSOCIATED CONTENT

Supporting Information

Nine supplementary figures. This material is available free of charge via the Internet at http://pubs.acs.org.

■ AUTHOR INFORMATION

Corresponding Authors

*Department of Medical Education, California Northstate University College of Medicine, 9700 W. Taron Dr., Elk Grove, CA 95757. E-mail: hugo.arias@cnucom.org. Telephone: (916) 686-7300. Fax: (916) 686-7310.

*Department of Anesthesiology, University of Pittsburgh School of Medicine, Pittsburgh, PA 15213. E-mail: tangp@anes.upmc.edu. Telephone: (412) 383-9798. Fax: (412) 648-8998.

Funding

This research was partially supported by National Institutes of Health Grant R01GM56257 (to P.T.) and by the TEAM research subsidy from the Foundation for Polish Science (to K.J.). In addition, the molecular modeling experiments were developed using the equipment purchased within the Project "The equipment of innovative laboratories doing research on new medicines used in the therapy of civilization and neoplastic diseases" within the Operational Program Development of Eastern Poland 2007−2013, Priority Axis I Modern Economy (to K.J.).

Notes

The authors declare no competing financial interest.

■ ABBREVIATIONS

AChR, nicotinic acetylcholine receptor; TMD, transmembrane domain; L, luminal; NL, nonluminal; LDAO, lauryldimethylamine-oxide; BS, binding saline; κ-BTx, κ-bungarotoxin; PCP, phencyclidine; RT, room temperature; BS, binding saline; K_i, inhibition constant; K_d, dissociation constant; IC_{50}, ligand concentration that produces 50% inhibition of binding; n_H, Hill coefficient; DMEM, Dulbecco's modified Eagle's medium; FBS, fetal bovine serum.

■ REFERENCES

(1) Shytle, R. D., Penny, E., Silver, A. A., Goldman, J., and Sanberg, P. R. (2002) Mecamylamine (Inversine): An old antihypertensive with new research directions. *J. Hum. Hypertens. 16*, 453−457.

(2) Shytle, R. D., Sheehan, D. V., Sanberg, P. R., and Arias, H. R. (2011) Neuronal nicotinic receptors as therapeutic targets for mood disorders. In *Pharmacology of Nicotinic Acetylcholine Receptors from the Basic and Therapeutic Perspectives* (Arias, H. R., Ed.) pp 187−198, Research Signpost, Kerala, India.

(3) Papke, R. L., Sanberg, P. R., and Shytle, R. D. (2001) Analysis of mecamylamine stereoisomers on human nicotinic receptor subtypes. *J. Pharmacol. Exp. Ther. 297*, 646−656.

(4) Fedorov, N. B., Benson, L. C., Graef, J., Lippiello, P. M., and Bencherif, M. (2009) Differential pharmacologies of mecamylamine enantiomers: Positive allosteric modulation and noncompetitive inhibition. *J. Pharmacol. Exp. Ther. 328*, 525−532.

(5) Newman, M. B., Manresa, J. J., Sanberg, P. R., and Shytle, R. D. (2001) Nicotine induced seizures blocked by mecamylamine and its stereoisomers. *Life Sci. 69*, 2583−2591.

(6) Lindsley, C. W. (2010) (S)-(+)-Mecamylamine (TC-5214): A neuronal nicotinic receptor modulator enters phase III trials as an adjunct treatment for Major Depressive Disorder (MDD). *ACS Chem. Neurosci. 1*, 530−531.

(7) Bondarenko, V., Mowrey, D., Tillman, T., Cui, T., Liu, L. T., Xu, Y., and Tang, P. (2012) NMR structures of the transmembrane domains of the α4β2 nAChR. *Biochim. Biophys. Acta 1818*, 1261−1268.

(8) Arias, H. R., Rosenberg, A., Targowska-Duda, K. M., Feuerbach, D., Jozwiak, K., Moaddel, R., and Weiner, I. W. (2010) Tricyclic antidepressants and mecamylamine bind to different sites in the human α4β2 nicotinic receptor ion channel. *Int. J. Biochem. Cell Biol. 42*, 1007−1018.

(9) Arias, H. R., Targowska-Duda, K. M., Sullivan, C. J., Feuerbach, D., Maciejewski, R., and Jozwiak, K. (2010) Different interaction between tricyclic antidepressants and mecamylamine with the human α3β4 nicotinic acetylcholine receptor. *Int. Neurochem. 56*, 642−649.

(10) Wishart, D. S., Bigam, C. G., Yao, J., Abildgaard, F., Dyson, H. J., Oldfield, E., Markley, J. L., and Sykes, B. D. (1995) ^{1}H, ^{13}C and ^{15}N chemical shift referencing in biomolecular NMR. *J. Biomol. NMR 6*, 135−140.

(11) Delaglio, F., Grzesiek, S., Vuister, G. W., Zhu, G., Pfeifer, J., and Bax, A. (1995) NMRPipe: A multidimensional spectral processing system based on UNIX pipes. *J. Biomol. NMR 6*, 277−293.

(12) Goddard, T. D., and Kneller, D. G. (2001) *SPARKY 3*, University of California, San Francisco.

(13) Gasteiger, E., Gattiker, A., Hoogland, C., Ivanyi, I., Appel, R. D., and Bairoch, A. (2003) ExPASy: The proteomics server for in-depth protein knowledge and analysis. *Nucleic Acids Res. 31*, 3784−3788.

(14) Arias, H. R. (2010) Positive and negative modulation of nicotinic receptors. *Adv. Protein Chem. Struct. Biol. 80*, 153−203.

(15) Moore, M. A., and McCarthy, M. P. (1995) Snake venom toxins, unlike smaller antagonists, appear to stabilize a resting state conformation of the nicotinic acetylcholine receptor. *Biochim. Biophys. Acta 1235*, 336−342.

(16) Cheng, Y., and Prusoff, W. H. (1973) Relationship between the inhibition constant (K_i) and the concentration of inhibitor which causes 50% inhibition (IC_{50}) of an enzymatic reaction. *Biochem. Pharmacol. 22*, 3099−3108.

(17) Schanker, L. S., Shore, P. A., Brodie, B. B., and Hogben, C. A. (1957) Absorption of drugs from the stomach. I. The rat. *J. Pharmacol. Exp. Ther. 120*, 528−539.

(18) Arias, H. R., Feuerbach, D., Targowska-Duda, K. M., and Jozwiak, K. (2013) Mecamylamine inhibits muscle nicotinic acetylcholine receptors by competitive and noncompetitive mechanisms. *OA Biochemistry 1*, 7.

(19) Arias, H. R., Feuerbach, D., Bhumireddy, P., and Ortells, M. O. (2010) Inhibitory mechanisms and binding site location for serotonin selective reuptake inhibitors on nicotinic acetylcholine receptors. *Int. J. Biochem. Cell Biol. 42*, 712−724.

(20) Arias, H. R., Feuerbach, D., Targowska-Duda, K. M., Aggarwal, S., Lapinsky, D. J., and Jozwiak, K. (2012) Structural and functional interaction of (±)-2-(N-tert-butylamino)-3′-iodo-4′-azidopropiophenone, a photoreactive bupropion derivative, with nicotinic acetylcholine receptors. *Neurochem. Int. 61*, 1433−1441.

(21) Arias, H. R., Bhumireddy, P., and Bouzat, C. (2006) Molecular mechanisms and binding site locations for noncompetitive antagonists of nicotinic acetylcholine receptors. *Int. J. Biochem. Cell Biol. 38*, 1254−1276.

(22) Hamouda, A. K., Chiara, D. C., Blanton, M. P., and Cohen, J. B. (2008) Probing the structure of the affinity-purified and lipid-reconstituted *Torpedo* nicotinic acetylcholine receptor. *Biochemistry 47*, 12787−12794.

(23) Giniatullin, R. A., Sokolova, E. M., Di Angelantonio, S., Skorinkin, A., Talantova, M. V., and Nistri, A. (2000) Rapid relief of block by mecamylamine of neuronal nicotinic acetylcholine receptors of rat chromaffin cells in vitro: An electrophysiological and modeling study. *Mol. Pharmacol. 58*, 778−787.

(24) Spurny, R., Billen, B., Howard, R. J., Brams, M., Debaveye, S., Price, K. L., Weston, D. A., Strelkov, S. V., Tytgat, J., Bertrand, S., Bertrand, D., Lummis, S. C., and Ulens, C. (2013) Multisite binding of a general anesthetic to the prokaryotic pentameric *Erwinia chrysanthemi* ligand-gated ion channel (ELIC). *J. Biol. Chem. 288*, 8355−8364.

(25) Bondarenko, V., Mowrey, D., Liu, L. T., Xu, Y., and Tang, P. (2013) NMR resolved multiple anesthetic binding sites in the TM domains of the α4β2 nAChR. *Biochim. Biophys. Acta 1828*, 398−404.

(26) Miyazawa, A., Fujiyoshi, Y., and Unwin, N. (2003) Structure and gating mechanism of the acetylcholine receptor pore. *Nature 423*, 949−955.

(27) Lester, H. A., Dibas, M. I., Dahan, D. S., Leite, J. F., and Dougherty, D. A. (2004) Cys-loop receptors: New twists and turns. *Trends Neurosci. 27*, 329−336.

(28) Cui, T., Canlas, C. G., Xu, Y., and Tang, P. (2010) Anesthetic effects on the structure and dynamics of the second transmembrane domains of nAChR α4β2. *Biochim. Biophys. Acta 1798*, 161−166.

(29) Jha, A., Purohit, P., and Auerbach, A. (2009) Energy and structure of the M2 helix in acetylcholine receptor-channel gating. *Biophys. J. 96*, 4075−4084.

(30) Bartos, M., Corradi, J., and Bouzat, C. (2009) Structural basis of activation of Cys-loop receptors: The extracellular−transmembrane interface as a coupling region. *Mol. Neurobiol. 40*, 236−252.
(31) Mowrey, D. D., Cui, T., Jia, Y., Ma, D., Makhov, A. M., Zhang, P., Tang, P., and Xu, Y. (2013) Open-channel structures of the human glycine receptor α1 full-length transmembrane domain. *Structure 21*, 1897−1904.
(32) Bondarenko, V., Mowrey, D. D., Tillman, T. S., Seyoum, E., Xu, Y., and Tang, P. (2014) NMR structures of the human α7 nAChR transmembrane domain and associated anesthetic binding sites. *Biochim. Biophys. Acta*, 10.1016/j.bbamem.2013.12.018.